Substrate suppression of thermal roughness in stacked supported bilayers

Curt M. DeCaro, Justin D. Berry,[*] and Laurence B. Lurio[†]

Department of Physics, Northern Illinois University, DeKalb, Illinois 60115, USA

Yicong Ma, Gang Chen, and Sunil Sinha

Department of Physics, University of Californiay, San Diego, La Jolla, California 92093, USA

Lobat Tayebi and Atul N. Parikh

Department of Applied Physics, University of California, Davis, Davis 95616, California, USA

Zhang Jiang and Alec R. Sandy

Advanced Photon Source, Argonne National Laboratory, Argonne, Illinois 60439, USA

We have fabricated a stack of five 1,2-dipalmitoyl-*sn*-3-phosphatidylethanolamine (DPPE) bilayers supported on a polished silicon substrate in excess water. The density profile of these stacks normal to the substrate was obtained through analysis of x-ray reflectivity. Near the substrate, we find the layer roughness and repeat spacing are both significantly smaller than values found in bulk multilayer systems. The reduced spacing and roughness result from suppression of lateral fluctuations due to the flat substrate boundary. The layer spacing decrease then occurs due to reduced Helfrich repulsion.

PACS number(s): 87.16.dj, 61.05.cm

I. INTRODUCTION

In recent years, supported phospholipid bilayers (SLBs) have become a topic of considerable interest because of their relevance to fundamental studies of membrane biology, soft matter, biophysics, and biosensor technology [1]. The planar, substrate-bound topology of SLBs confers advantages for characterizing the structural properties of lipid membranes and membrane protein interactions using probes such as atomic force microscopy or x-ray and neutron scattering, which require oriented systems. There are also technological advantages of being able to place a biomimetic membrane on semiconductor surfaces, which could facilitate applications in biosensors and biocompatible coatings [2]. The properties of SLBs can, however, differ from alternate model membrane configurations such as bilayers in free-floating vesicles or lyotropic liquid-crystalline mesophases of lipid bilayers. For example, in phase-separating bilayers which are part of vesicles, the domains are generally much larger, having microscopic dimensions, than in SLBs, which show nanoscale domains [3]. Furthermore, even if the in-plane mobility of SLBs is not significantly reduced, fluctuations of SLBs normal to the interface are expected to be severely restricted relative to other systems. Such fluctuations, however, play an important role in membrane function in cellular processes such as the initiation of budding of small vesicles or in proximity-mediated reactions such as membrane fusion [4,5].

There have been a number of x-ray scattering measurements from SLBs on silicon wafers [6]. Recently measurements have also been made on stacks of two lipid bilayers [7], where the membrane stacks were prepared using a Langmuir-Blodget Langmuir-Schaffer method pioneered by Charitat *et al*. [8]. These two bilayer stacks are often referred to as "floating" membrane systems, due to the reduced coupling of the top layer to the substrate. The method of Charitat *et al*. has been employed using a number of fully saturated lipids such as 1,2-dipalmitoyl-*sn*-3-phosphatidylcholine (DPPC) [8], 1,2-dimyristoyl-*sn*-3-phosphatidylcholine (DMPC) [9], 1,2-distearoyl-*sn*-3-phosphatidylcholine (DSPC) [7,10], and 1,2-dipalmitoyl-*sn*-3-phosphatidylethanolamine (DPPE) [11]. In the current work, we have extended this method to the deposition of five bilayers of DPPE on a solid Si support. A model of the density profile of the resulting stack normal to the substrate is then obtained from x-ray specular reflectivity measurements.

II. EXPERIMENTAL PROCEDURES

Bilayer stacks were prepared using DPPE acquired from a commercial source (Avanti Polor Lipids, Alabaster, AL) and used without further purification. The lipids were shipped in a chloroform/methanol/water mixture (at a concentration of 10 mg/ml) and diluted with chloroform to 0.5 mg/ml for spreading on the subphase of a Langmuir-Blodget (LB) trough. Multiple leaflets of lipid were deposited on top of polished silicon substrates using a Langmuir-Blodget, Langmuir-Schaffer (LB/LS) dipping method. Protocols for depositing up to four leaflets have been previously established by Charitat *et al*. [8] and were followed in the present case. Subsequent leaflets were deposited by a repeated process of subphase aspiration, monolayer redeposition on the subphase, and then the LB/LS dipping procedure. During the LB steps the extraction/submersion rate was 5 mm/min, while the LS depositions were 1 mm/min. To reduce bilayer defects during formation due to external vibrations, the trough was placed

---

[*]Present address: Department of Physiology and Biophysics, Boston University School of Medicine, 700 Albany St., Boston, MA 02118-2526, USA.

[†]llurio@nui.edu

on a Halcyonics Vario Basic 40 (MOD-2 type) antivibration table. This procedure could be repeated to deposit up to five bilayers, which was the largest stack attempted.

Since the ultimate spatial resolution of the x-ray measurements is limited by the surface roughness of the substrate it was necessary to use flat and highly polished substrates. Silicon substrates (2 mm thick) were custom ordered from SESO in France with a nominal rms surface roughness of 120 pm. The Si surface was cleaned by sonication in chloroform and methanol and then via uv-ozone cleaning [12].

X-ray specular reflectivity measurements were performed at the Advanced Photon Source 8-IDI beamline at Argonne National Laboratory, using photons at 22.05 keV. All measurements were made in excess water. The multilayers were measured at 25 °C. Successive specular scans were identical, confirming that the samples were not radiation damaged. Measurements were also repeated and confirmed using an in-house spectrometer, using molybdenum K-α radiation at 17.5 keV.

III. RESULTS

Specular reflectivity from a stack of five bilayers is shown in Fig. 1 plotted as a function of $Q = 4\pi \sin(\theta)/\lambda$. Here 2θ is the angle of the scattered beam relative to the incident beam and λ is the x-ray wavelength. We have inverted the real-space density profile from the reflectivity data using direct Fourier inversion. This technique has been employed previously by Sanyal *et al.* [13] and Marschand *et al.* [14]. The basis of this method is that at large wave vector, Q, where refraction effects can be neglected, the specular reflectivity is proportional to the absolute square of the Fourier transform of the average density profile normal to the surface. Under these conditions the scattering can be modeled by the so-called master formula for specular reflection:

$$R/R_F = \left| \frac{1}{\rho_{e,\infty}} \int_{-\infty}^{\infty} \frac{\partial \rho_e(z)}{\partial z} e^{iQ'z} dz \right|^2. \quad (1)$$

Here ρ_e is the effective electron density within the material, $\rho_{e,\infty}$ is the electron density deep within the the substrate, z is the position along the substrate normal, and Q' is the wave vector corrected for refraction inside the material.

If the phase of the reverse transform were known, inversion of the profile would only require a reverse Fourier transform. Since the phase is not known, we employ an iterative method to recover the phase. Initially the phase is assumed to be zero, and the measured reflectivity is reverse transformed with this phase, providing a guess at a real-space profile. This real-space profile is then subject to physical constraints of positive density and finite extent. After imposing constraints the Fourier transform of this profile is used to obtain the phase guess for the next inversion of the *measured* reflectivity data. This process is repeated until convergence is obtained. The results of this inversion are shown as the fits in Fig. 1 and the resulting real-space profile is given in Fig. 2.

While the direct-inversion profile yields an excellent fit to the data its physical significance can be difficult to interpret. As an alternative method of modeling the data, we created a real-space density model based on modifications to the density profile measured for the bulk smectic phase by x-ray diffraction [15]. The model has three components. First, reported real-space Fourier components of bulk DPPE multilayers in excess water were used to create a repeating density profile. This profile was then truncated and set to the water density for any distance from the substrate larger than five times the layer
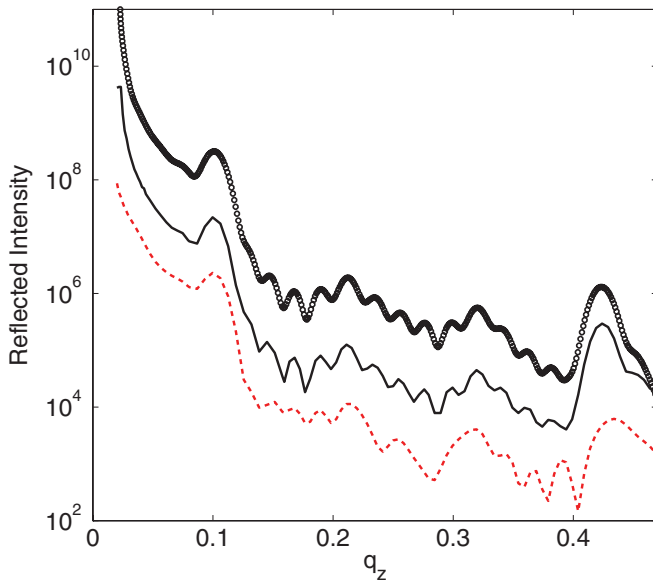

FIG. 1. (Color online) Measured reflectivity from five DPPE bilayers (black circles), direct-inversion fit (solid black line), and model generated reflectivity (red dashed line) Successive data are offset by a factor of 10.
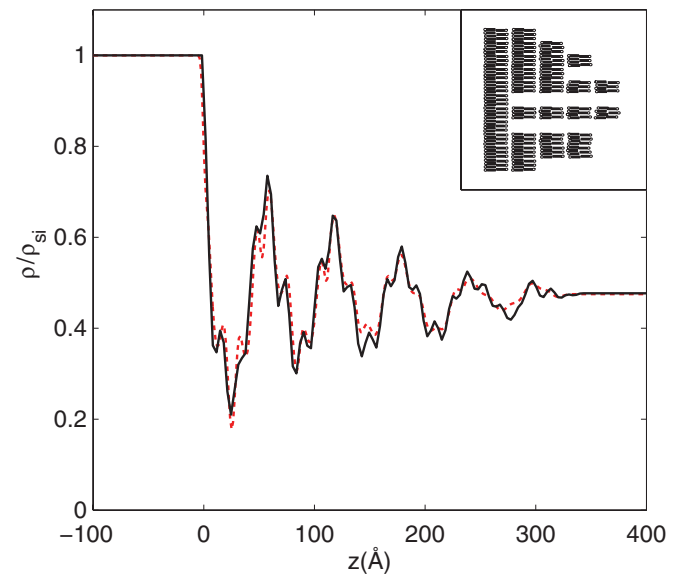

FIG. 2. (Color online) Directly inverted (solid line) real-space density profile from a stack of five DPPE bilayers and the real-space model (dashed line, red) of a supported stack of five bilayers. The profile shows densities normal to the plane of the substrate. The substrate itself occupies space $z < 0$. Eventually ($z \approx 350$ Å) the lamellae terminate to the density of water. A cartoon of the model is shown in the inset.

TABLE I. Fourier components used to construct the bulk DPPE profile, from McIntosh [15].

Fourier order	Structure amplitude	Phase
1	1.00	π
2	0.11	0
3	0.13	π
4	0.55	π
5	0	0
6	0.15	π

spacing. This profile was then modified by four operations: (1) stretching of the profile to account for variation of the layer spacing with distance from the substrate, (2) convolution of the profile with a roughness function to account for fluctuations at the membrane interfaces, (3) multiplication of the profile by a partial occupation factor to account for incomplete layer deposition, and (4) multiplication of each leaflet of the bilayer by a factor to account for different packing density in the top and bottom leaflets.

To construct the initial bilayer model we begin with the Fourier density components obtained from diffraction data:

$$\rho(z) = C \sum_h \sqrt{h^2 I(h)} \phi(h) \cos(2\pi z h/d). \qquad (2)$$

Here z is the distance along the substrate surface normal direction and C is an overall diffraction scale factor. The amplitudes $I(h)$ and phase factors $\phi(h)$ were obtained from McIntosh [15] and are reproduced here in Table I. The density of each successive leaflet of the stack relative to water, ρ/ρ_{water}, was also allowed to vary to account for either incomplete coverage or varying density of the leaflets.

To account for roughness of the membrane interface, the entire density profile was then subjected to convolution by a z-dependent roughness factor $\sigma(z)$. This included contributions from both the substrate roughness, 1.5 Å confirmed by independent reflectometry measurement, and the film roughness $\sigma_{\text{film}}(z)$. The factor $\sigma_{\text{film}}(z)$ was treated as a step function with five steps, each of length equal to the d spacing of the respective bilayer and a variable height. The five amplitudes were allowed to vary independently to achieve convergence.

This model contains a number of free parameters. In order to use the periodic intensity variation from the bulk diffraction data an overall intensity scale factor needs to be included. Furthermore, the distance from the substrate surface to the first multilayer (e.g., the phase of the layers relative to the

substrate) must be defined. We find that the optimal offset corresponds to the beginning of the bilayer, defined as 2.0 Å in front of the center of the first phosphate head group, being coincident with the substrate interface. The variation of the d spacing of the layers was assumed to be a quadratic variation from an initial d spacing to a final d spacing. The ratio of the density of the inner and outer leaflets was another adjustable parameter. All the layers were allowed to have independent transfer ratios. An additional two parameters were needed to account for angular offset and normalization uncertainties of the x-ray data.

The fit parameters were varied until the model-calculated reflectivity converged with the data. The fit from this model is shown as the lower curve in Fig. 1 and the resulting real-space profile in Fig. 2. The real-space profile resulting from this fit is very close to the direct-inversion result. However the quality of the fit to the reflectivity data in the Q space is significantly poorer than the direct-inversion result. The maxima and minima are out of phase at Q values of 0.15, 0.29, and 0.41. Furthermore, the average fractional error $(I_{\text{fit}} - I_{\text{meas}})/I_{\text{meas}}$ was 13% for the fit as compared with 0.3% for the direct-inversion profile. Based on this disagreement, we assume that where the real-space densities differ between the direct inversion and fit results, the direct-inversion real-space profile should be trusted in preference to the fit. However, an inspection of Fig. 2 shows that the fit gives a nearly identical real-space profile. Apparently, even small errors in the real-space profile can generate significant deviations in the fit to the reflectivity. Nevertheless, the fitting method clearly captures the most important features of the real-space profile and is a convenient way to quantify the characteristics of the profile. In the absence of the direct-inversion result it would be difficult to know how much to trust the model fit. However, since the direct-inversion result is an excellent model of the scattering and since the fit results show features very similar to those of the direct-inversion result in real space, we believe that the fit parameters are significant. Since these parameters allow us to characterize the trends in the data conveniently, we focus our discussion on the parameters from the fit results.

The parameters obtained from this fit are given in Table II. These fits indicate that the layer spacing contracts by nearly 8 Å from its value of 62–63 Å at the middle layers (which is equal to the bulk value) and expands by 7 Å at the outermost layer. The interfacial roughness, which can be calculated for each layer using Eq. (3) and the model parameters, also increases systematically as a function of distance from the substrate, from 0.8 to 3.5 Å. The transfer ratios were 0.75 ± 0.03. This value is substantially smaller than that predicted from pressure

TABLE II. Fit parameters used to model the reflectivity data for the stack of five DPPE bilayers in the gel phase. Transfer ratios are given relative to the supporting layer coverage, rather than as absolute coverage.

Layer	d Spacing (Å)	Roughness (Å)	Layer occupation	Other parameters
1	52.7 ± 0.2	0.82		Upper leaflet ratio 1.05 ± 0.01
2	59.1 ± 0.3	0.64	0.75	Lower leaflet ratio 0.89 ± 0.01
3	61.1 ± 0.5	2.58	0.66	
4	62.7 ± 0.7	3.15	0.47	Diffraction scale factor = 5.4
5	70.1 ± 0.9	3.68	0.26	

area isotherms, indicating that the packing density on the substrate may not be the same as that at the liquid-vapor interface.

IV. DISCUSSION

Analysis of the reflectivity shows a systematic decrease in the bilayer roughness with proximity to the substrate. This decreased roughness occurs with a corresponding decrease in average layer spacing. Qualitatively, we can understand the decreased roughness via the following mechanism. For the bilayer unit directly adjacent to the substrate, the suppression of roughness may stem from a variety of substrate-induced perturbations. The competition between intermembrane interactions including short-range, water-mediated hydration repulsion and long-range van der Waals attraction, which primarily determine interlamellar spacing and interfacial roughness, are substantially altered in the vicinity of a rigid substrate. Small differences in molecular packing due to substrate-induced tension may also introduce additional perturbations in the dipolar head-group interactions, which contribute to surface roughness.

Regarding the upper floating layers, since the lipid molecules are not free to easily move between layers, fluctuations in the membrane position can only occur through compression of the bilayers. Since bilayer compression involves an energy cost, the suppression of fluctuations propagates into the upper layers. A quantitative analysis of the effect of a solid surface on the fluctuations in lipid bilayer stacks was worked out by Constantin *et al.* [16] who applied this to the study of spin-cast lipid films. They derived a formula for the roughness as a function of distance from the interface under the assumption that the surface tension of the lipid-water interface was negligible. Their result is given by

$$\sigma^2(z) = \eta(d/\pi)^2 \sum_{n=1}^{N} \frac{1}{2n-1} \sin^2\left(\frac{(2n-1)\pi z}{2Nd}\right).$$

Here $\eta = \pi k_B T / 2\sqrt{KB}d^2$, d is the thickness of a bilayer, k_B is the Boltzmann's constant, T is the temperature, B is the bulk compressibility, K is the bulk bending modulus, and N is the number of layers. Petrache *et al.* [17], based on the analysis of the variation of d spacing with osmotic pressure for bulk DPPE, provides a range of values for K and B of $K = 0.5$–2×10^{-12} erg and $B \approx 10^{13}$ erg/cm^4. We have plotted the predictions of this formula vs the best fit values of $\sigma(z)$ in Fig. 3. In order to distinguish thermal roughness from substrate-induced roughness we have subtracted the substrate roughness of $\sigma_{\text{sub}} = 1.5$ Å in quadrature from the fit values. As can be seen from the figure, this model yields remarkably good agreement for the outermost layers. The discrepancy in the first two layers may be due to the additional suppression of fluctuations due to the van der Waals field.

A plausible explanation for the reduction in layer spacing near the substrate is that this results from the reduced fluctuation of the membrane. Helfrich [18] has previously calculated that when membranes are in close proximity to a solid boundary, or, alternatively, another membrane, then there is a reduction in the entropy available to the membrane due to the reduced volume for fluctuations. This leads to an effective repulsive force between membranes, which has been dubbed
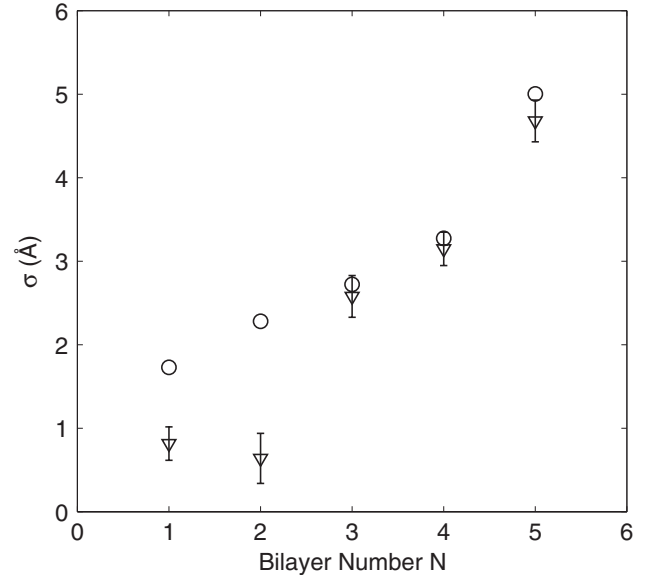

FIG. 3. Theoretical height-height correlation function derived by Constantin *et al.* [16] (circles) and the measured film roughness (inverted triangles) at lamellar interfaces. The measured film roughness shown is before convolution with the substrate roughness. Values of elastic constants used are $K = 2.2 \times 10^{-12}$ erg and $B = 2.3 \times 10^{13}$ erg/cm^4.

the Helfrich repulsion. In the present case in addition to the change in entropy predicted by Helfrich, there is an energy cost associated with fluctuations, since the proximity to a flat substrate requires fluctuations to compress the membranes. Thus the increase in free energy due to the loss of volume for fluctuations is not as significant as in the case for bulk multilayers and the Helfrich repulsion should be reduced. This would then lead to smaller values for the layer d spacings.

When the stacks of membranes were heated above the liquid-gel transition temperature they were found to unbind from the substrate. This effect can also be explained from the effect of the Helfrich repulsion. A decrease in the bending modulus upon the transition from gel to liquid should result in larger fluctuations and a stronger Helfrich repulsion resulting in unbinding. The dramatic increase in d spacing of the top film bilayer is also consistent with this hypothesis, since the energy cost for fluctuations of the top layer should only be approximately half that of the other layers.

There are additional interactions between membranes beyond the van der Waals interactions and Helfrich undulations discussed here. These include hydration interactions and dipole interactions between charges in the water and in the phospholipids [17,19,20]. However, these interactions can effectively be taken into account by the values of the bulk compressibility B and the bending modulus K. In particular, there is no reason why these interactions should depend on the distance from the substrate. On the other hand, the substrate-bilayer van der Waals interaction and the Helfrich undulations should show significant variations with distance from the substrate as discussed above. Since the Helfrich undulations are the more dominant of these two interactions we believe it is justified to interpret the variation in layer spacing with substrate distance in terms of this effective force.

One unexpected result from the reflectivity fits is that the densities of the lower leaflets (done by the LB process) are systematically higher than those of the upper leaflets (done by the LS process). Since a planar lipid monolayer is not stable in excess water, this implies a difference in transferred packing density between LB and LS leaflets rather than partial-coverage leaflets. Most likely, successive bilayers exhibit successively smaller total coverage, and the two leaflets which compose the bilayer exhibit different packing densities. It is also notable that the addition of a water layer between the substrate and the first leaflet was not required to achieve fit convergence. In fact, the addition of such a layer prevented fit convergence with measured reflectivity.

One important concern regarding the extraction of a real-space profile from measured reflectivity data is the uniqueness of the solution. We note that there are strong similarities in the real-space profiles obtained by the model fit and the direct inversion even though the only information that went into the direct inversion was an estimate of the layer thickness and the relative density of water and silicon. This very close agreement gives support to the argument that there is not another very different solution to the reflectivity. The fact, however, that the direct-inversion result gives a better match to the reflectivity indicates that its real-space profile may be somewhat more accurate. In particular the model deviates from the direct-inversion profile most strongly in the first and last layers. This may indicate that the perturbations associated with the substrate and the free surface are too strong to be completely modeled by the modifications to the bulk structure used in our model.

In conclusion, we demonstrate here a method to deposit a discrete and controllable number of lipid bilayer stacks on a silicon substrate. We show that direct inversion of specular reflectivity yields a physically plausible structure for the layers and that the data can also be fit using a model for this layer density based on modifications to the bulk layer profile obtained using diffraction. While this fit is of somewhat lower quality than the direct-inversion fit, it has the advantage that parameters such as layer spacing, roughness, and occupation factor can be directly obtained. These parameter values agree quantitatively with the expectations for the variation of layer thermal broadening and agree qualitatively with the expectation that Helfrich forces will yield a reduced layer spacing when the thermal roughness is suppressed. In the first two bilayers, however, the thermal roughness appears to be completely suppressed, which likely indicates that very close to the substrate van der Waals interactions need to be taken into account.

[1] E. T. Castellana and P. S. Cremer, Surf. Sci. Rep. **61**, 429 (2006).

[2] A. N. Parikh and J. T. Groves, MRS Bull. **31**, 507 (2006).

[3] S. L. Veatch and S. L. Keller, Biochim. Biophys. Acta **1746**, 172 (2005).

[4] A. Chanturiya, L. V. Chernomordik, and J. Zimmerberg, Proc. Nat. Acad. Sci. USA **94**, 14423 (1997).

[5] L. Yang and H. W. Huang, Science **297**, 1877 (2002).

[6] E. Novakova, K. Giewekemeyer, and T. Salditt, Phys. Rev. E **74**, 51911 (2006).

[7] J. Daillant, E. Bellet-Amalric, A. Braslau, T. Charitat, G. Fragneto, F. Graner, S. Mora, F. Rieutord, and B. Stidder, Proc. Natl. Acad. Sci. USA **102**, 11639 (2005).

[8] T. Charitat, E. Bellet-Amalric, G. Fragneto, and F. Graner, Eur. Phys. J. B **8**, 583 (1999).

[9] A. V. Hughes, S. J. Roser, M. Gerstenberg, A. Goldar, B. Stidder, R. Feidenhans'l, and J. Bradshaw, Langmuir **18**, 8161 (2002).

[10] G. Fragneto, T. Charitat, F. Graner, K. Mecke, L. Perino-Gallice, and E. Bellet-Amalric, Europhys. Lett. **53**, 100 (2001).

[11] B. Stidder, G. Fragneto, and S. J. Roser, Soft Matter **3**, 214 (2007).

[12] J. R. Vig, J. Vac. Sci. Technol. A **3**, 1027 (1984).

[13] M. K. Sanyal, S. Hazra, J. K. Basu, and A. Datta, Phys. Rev. B **58**, R4258 (1998).

[14] L. W. Marschand, M. Brown, L. B. Lurio, B. M. Law, S. Uran, I. Kuzmenko, and T. Gog, Phys. Rev. E **72**, 011509 (2005).

[15] T. J. McIntosh, Biophys. J. **29**, 237 (1980).

[16] D. Constantin, U. Mennicke, C. Li, and T. Salditt, Eur. Phys. J. E **12**, 283 (2003).

[17] H. I. Petrache, N. Gouliaev, S. Tristram-Nagle, R. Zhang, R. M. Suter, and J. F. Nagle, Phys. Rev. E **57**, 7014 (1998).

[18] W. Helfrich, Z. Naturforsch. **33a**, 305 (1978).

[19] R. E. Goldstein and S. Leibler, Phys. Rev. Lett. **61**, 2213 (1988).

[20] R. E. Goldstein and S. Leibler, Phys. Rev. A **40**, 1025 (1989).